Available online at www.sciencedirect.com
ScienceDirect
Carbohydrate Polymers 72 (2008) 410–418
Carbohydrate Polymers
www.elsevier.com/locate/carbpol

Intermolecular interactions in electrospun collagen–chitosan complex nanofibers

Zonggang Chen [a,b], Xiumei Mo [a,*], Chuanglong He [a], Hongsheng Wang [a]

[a] *Institute of Biological Science and Biotechnology, Donghua University, Shanghai 201620, China*
[b] *College of Chemistry and Chemical Engineering, Donghua University, Shanghai 201620, China*

Received 16 April 2007; received in revised form 29 August 2007; accepted 11 September 2007
Available online 5 November 2007

Abstract

The collagen–chitosan complex nanofibers have been prepared here by electrospinning. Intermolecular interactions in electrospun collagen–chitosan complex fibers have been studied by Fourier transform infrared spectroscopy (FT-IR), differential scanning calorimetry (DSC) and the mechanical measurements of single ultrafine fiber. It was found that the –OH group, the $-NH_2$ group and the amide I, II and III characteristic absorption bands in FT-IR spectra of electrospun collagen and chitosan blends were shifted and modified with the difference of chitosan content in electrospun fibers. DSC measurements showed the existence of intermolecular interactions enthalpy between collagen and chitosan of electrospun fibers. The mechanical measurements of single nanofiber showed that intermolecular interactions varied with various chitosan content in electrospun fibers.

The results have shown that intermoleculars interactions exist in electrospun collagen–chitosan complex fibers. These interactions make collagen and chitosan be miscible at the molecular level. Electrospinning of collagen and chitosan blends may give the possibility of producing new materials for potential biomedical applications.

Keywords: Collagen; Chitosan; Electrospinning; Intermolecular interaction

1. Introduction

At present, one of focuses studied in biomaterial fields is how to prepare the mimic extracellular matrices whose components and structures are analogous to those of the native extracellular matrices (ECMs). These mimic ECMs can improve the biocompatibility and functionality of biomaterials. Because the native ECMs are the complex of protein and polysaccharide with nanofibrous porous structure, the complex of protein and polysaccharide, especially, the collagen and chitosan complex can be used to mimic the ECMs of native tissues.

Collagen is the most abundant structural protein found in the animal body such as in skin, tendon, cartilage and bone (Cui & Feng, 2004). Owing to a wealth of merits such as its biological origin, non-immunogenicity, excellent biocompatibility and biodegradability, collagen has been widely used as biomaterial in the pharmaceutical and medical fields as sealants for vascular (Marois et al., 1995), carrier for drug delivery (Ky, Liu, Marumoto, Castaneda, & Slowinska, 2006), dressings for wound healing (Gomathi, Gopinath, Ahmed, & Jayakumar, 2003) and tissue engineering scaffold (Matthews, Wnek, Simpson, & Bowlin, 2002). Chitosan is only a basic natural polysaccharide derived from chitin, which is the second natural resource only inferior to the cellulose. Because of its abundant production in nature, excellent biocompatibility, appropriate biodegradability, excellent physicochemical properties, and commercial availability at relatively low cost, it has also been widely used as biomaterials in the pharmaceutical

* Corresponding author. Tel.: +86 021 67792653; fax: +86 021 67792647.
E-mail address: xmm@dhu.edu.cn (X. Mo).

0144-8617/$ - see front matter © 2007 Elsevier Ltd. All rights reserved.
doi:10.1016/j.carbpol.2007.09.018

and medical fields. (Huang & Jiang, 2006; Huang, Onyeri, Siewe, Moshfeghian, & Madihally, 2005).

The collagen and chitosan blends have been widely used as biomaterials in the pharmaceutical and medical fields recently (Chen, Wang, Chen, Ho, & Sheu, 2006; Ma et al., 2003). They are prepared by cross-linking (Wang et al., 2003), wet/dry spinning (Hirano, Zhang, Nakagawa, & Miyata, 2000) and freeze-drying (Lee, Kim, Chong, & Lee, 2004) and the fabric of blends is in a macroscopic scale. However, the structure of the ECMs is at the nanoscale (Silver & Christiansen, 1999). These native ECMs act as structural elements to hold and bring cells together in tissues, control the tissue structure and regulate cell phenotypes (Alberts et al., 1994). Recently, it has been found that the nanofibrous structure can improve the regeneration of tissues *in vitro* including bone, cartilage, cardiovascular tissue, nerve and bladder as human cells can attach and organize well around fibers with diameter smaller than those of the cells (Laurencin, Ambrosio, Borden, & Cooper, 1999). It can also minimize scars in tissues (Webster, Waid, McKenzie, Price, & Ejiofor, 2004). In order to improve the biocompatibility and functions of biomaterials, it is essential for collagen and chitosan blends to mimic the nanofibrous structure of the native ECMs.

Recently, the collagen–chitosan complex nanofibers have been prepared by electrospinning in our lab (Chen, Mo, & Qing, 2006, 2007). Electrospinning is to spin the fibers in nano-scale by electrostatic force (Huang, Zhang, Kotaki, & Ramakrishna, 2003). In the pharmaceutical and medical fields, this technique has been used to make wound dressings (Khil, Cha, Kim, Kim, & Bhattarai, 2003), drug delivery materials (Zeng et al., 2003) and tissue engineering scaffolds (Jin, Fridrikh, Rutledge, & Kaplan, 2002). So the electrospun collagen–chitosan nanofibers may represent a potential tissue engineering scaffold and a promising functional biomaterial such as wound dressings and carrier for drug delivery.

For a blend, an important aspect of the properties is the miscibility of its components. Miscibility in polymer blends is assigned to specific interactions between polymeric components. The most common interactions in the blends are hydrogen bond, ionic and dipole, p-electrons and charge-transfer complexes (Sionkowska, Wisniewski, Skopinska, Kennedy, & Wess, 2004). Most polymer blends are immiscible each other due to the absence of specific interactions, however, chitosan can form complex with collagen (Mo, 1997; Sionkowska et al., 2004). The influence of chitosan on physicochemical and biochemical properties of collagen and intermolecular interactions in collagen and chitosan blends have been studied previously (Domard & Taravel, 1995; Taravel & Domard, 1993, 1996). It has been shown that chitosan can modify the biological and mechanical properties of collagen, moreover, the formation of polyanion–polycation complex and new hydrogen bonding networks between collagen and chitosan were observed (Domard & Taravel, 1995). However, these studies were performed in macroscopic collagen and chitosan blended casting membrane obtained by casting the solution onto glass plate and evaporating the solvent. Intermolecular interactions in electrospun collagen–chitosan nanofibers have not been reported. From the foregoing, further physical and structural characterization of the collagen–chitosan nanofibers is required to develop novel biomaterial properties that allow a more extensive characterization of the effect of miscibility at the molecular level. Here, electrospinning of collagen–chitosan nanofibers was studied further and a single nanofiber was spun and collected successfully. We used FT-IR, DSC and the mechanical measurements of a single nanofiber to produce a better insight into intermolecular interactions of collagen and chitosan in electrospun nanofibers.

2. Materials and methods

2.1. Materials

Collagen I (mol. wt, $0.8–1 \times 10^5$ Da) was purchased from Sichuan Ming-rang Bio-Tech Co. Ltd. (China) while Chitosan (85%, deacetylated, M_η, about 10^6) was purchased from Ji Nan Haidebei Marine Bioengineering Co. Ltd. (China). Two kinds of solvents, 1,1,1,3,3,3-hexafluoroisopropanol (HFP) from Fluorochem Ltd. (United Kingdom) and Trifluoroacetic acid (TFA) from Sinopharm Chemical Reagent Co., Ltd. (China) were used to dissolve the collagen, chitosan and their blends.

2.2. Electrospinning

Collagen, chitosan and their blends with various chitosan content were dissolved in HFP/TFA (v/v, 90/10) at a concentration of 8% (g/ml). These prepared solutions were then used in the electrospinning experiments.

The electrospinning experiments were performed at room temperature. The polymer solution was placed into a 1 ml syringe with a needle having an inner diameter of 0.46 mm. A clamp connected the high voltage power supplier (which can supply positive voltage from 0 to 30 kV) (Institute of Beijing High Voltage Technology, China) to the needle. A piece of aluminum foil glued onto the cardboard with double-side tapes was placed at about 130 mm directly below the needle and acted as grounded collector. The polymer jets generated from the needle by the high voltage field formed the ultrafine fibers and fibrous membrane at the grounded collector. The applied voltage and feed rate of the solution were fixed at 16 kV and 0.8 ml/h, respectively.

2.3. Scanning electron microscopy analysis

The morphologies of the electrospun fibers and membrane were observed under a scanning electron microscope (SEM) (Quanta FEG 200, FEI Company, The

Netherlands) at an accelerating voltage of 10 or 15 kV. Prior to scanning under the SEM, the samples were sputter coated for 90 s with gold using a JEOL JFC-1200 fine coater. Based on the SEM photographs, the diameters of fibers were analyzed using image visualization software Adobe Photoshop.

2.4. Fourier transform-infrared spectroscopy analysis

FT-IR studies were carried out on compressed films containing KBr pellets and products using a FT-IR spectrophotometer (Avatar380, USA). All spectra were recorded by absorption mode at 2 cm^{-1} interval and in the wavelength range of 3800–600 cm^{-1} wave numbers.

2.5. Differential scanning calorimetry analysis

The thermal properties of the electrospun fibers were measured by a TA Instruments DSC-822 Differential Scanning Calorimeter (METTLER TOLEDO Company, Switzerland) in a temperature range from 0 °C to 200 °C at a heating rate of 10 °C/min.

2.6. X-ray diffraction analysis analysis

X-ray diffraction (XRD) analysis was conducted using a D/Max-2550 PC X-ray diffractometer (Rigaku, Japan) with Cu K α-radiation.

2.7. Collection and tensile test of a single ultrafine fiber

A single polymer ultrafine fiber is so weak that any direct touch on the fibers during manipulation can damage the fiber. As such, extreme care must be taken in collecting and testing the tensile specimens in order to avoid any damage. In this study, the equipment for collecting the fibers comprises a rectangular aluminum or copper frame which collects the fibers in the electric field as shown in Fig. 1.

In electrospinning, the specimens were collected as follows: a rectangular aluminum or copper frame was placed 60° to the horizontal surface between the spinneret and the grounded collector. During electrospinning, several strands of fibers were deposited across the frame as shown in Fig. 1A. The frame (a) was attached to the aluminum frame for collection of a single fiber. The double-sided tapes on the frame allowed the fiber to be adhered to the frame as shown in Fig. 1C. The frame (a) was then separated into the plastic frame (b) and the metal frame (c). The single fiber on the plastic frame (b) was used to perform the tensile test and the single fiber on the metal frame (c) was used to measure the diameter of the fiber as shown Fig. 1D.

Collection of fibers and tensile tests were carried out on the same day to minimize the effects of environment. A commercial nano tensile testing system (Nano Bionix System, MTS, TN, USA) was used to conduct the tensile test.

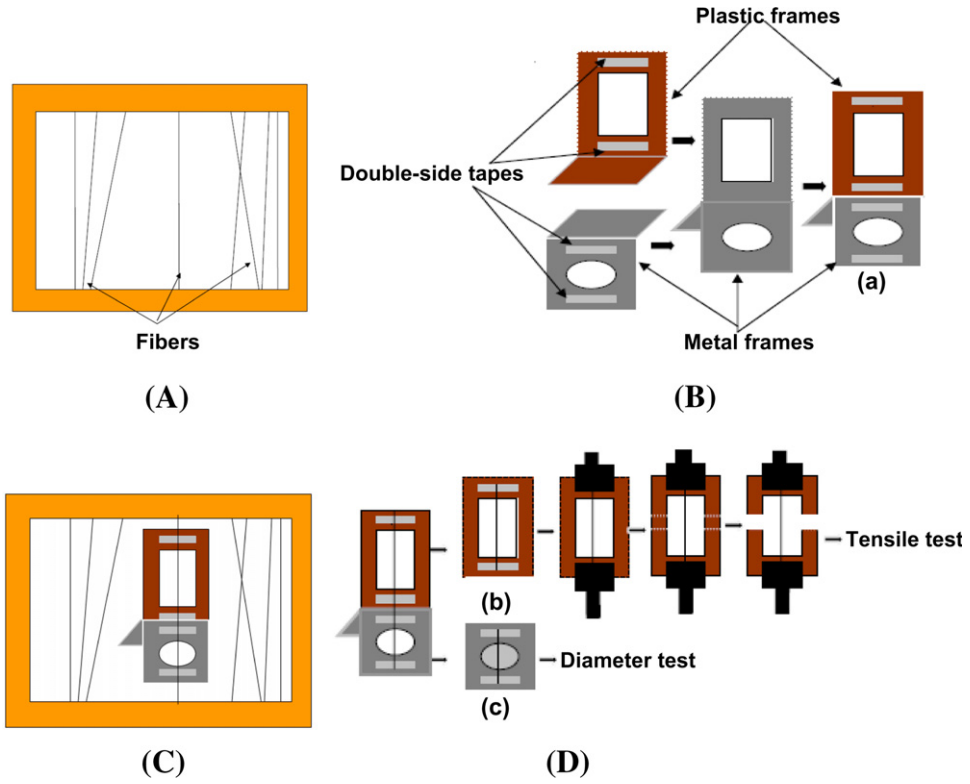

Fig. 1. Collection of a single fiber. (A) A rectangular aluminum or copper template was used to collect the fibers; (B) collecting tools for a single fiber; (C) collection of a single fiber; (D) tensile test of a single fiber.

The test was performed in ambient temperature at 20 °C and humidity of 65%. The gauge length (10 mm) of the electrospun single fiber was determined by the gap between the parallel strips of the plastic frame. The samples were mounted on the nano tensile tester. The plastic frame was cut along the discontinuous lines before stretching the fiber as shown in Fig. 1D. Samples were stretched to failure at a low strain rate of 1%/s.

3. Results and discussion

3.1. Solvent selection

The biggest challenge for collagen–chitosan electrospinning is to find a suitable solvent. 1,1,1,3,3,3-hexafluoroisopropanol (HFP) was successfully used as solvent for electrospinning of collagen (Matthews et al., 2002). An attempt was made to dissolve chitosan in HFP, but a gel was formed and no fiber could be electrospun due to high viscosity. In the literature, it was reported that chitosan could be dissolved in trifluoroacetic acid (TFA) by the amino groups on chitosan forming salts with TFA (Hasegawa, Isogai, Onabe, & Usuda, 1992). Hence, TFA was added to the solution of chitosan in HFP to improve chitosan solubility. As a result, the viscosity of the solution decreased significantly and the formed solution was able to be electrospun into fibers. However, some collagen would be decomposed if too much TFA was used in the solution. Hence, a mixture of HFP and TFA with with only 10% TFA content was selected as an appropriate solvent for electrospinning of chitosan and collagen blends.

3.2. Morphologies of a single ultrafine fiber and membrane

Fig. 2a showed a SEM micrograph of a single electrospun collagen–chitosan fiber and Fig. 2b showed a SEM micrograph of electrospun collagen–chitosan complex fibrous membrane with chitosan content of 50% in the electrospun fibers. The fiber diameters in the membrane range from nanometer to micrometer size, but the single fiber collected here is about one or several micrometers in diameter. A thinner single fibers is difficulty to be collected because they may be broken during collection.

3.3. Study of Fourier transform infrared spectroscopy

The interactions between electrospun collagen and chitosan have been confirmed by FT-IR spectra of collagen, chitosan, and their blends. FT-IR is a very powerful technique to detect the intermolecular interactions between two polymers. Besides new created functional group by chemical reaction between polymers, the intermolecular interactions through hydrogen bonding can also be characterized by FT-IR, because the specific interactions affects the local electron density and the corresponding frequency shift can be observed (Kaminska & Sionkowska, 1996).

3.2.1. Effect of solvent on collagen and chitosan

The bought raw collagen and its casting membrane from collagen solution in HFP/TFA (v/v, 90/10) were measured by FT-IR and given their FT-IR spectra as in Fig. 3.

Collagen has the characteristic absorption bands at 1660, 1550 and 1240 cm^{-1}, which represent the amide I, II and III bands of collagen. Amide I absorption arises predominantly from protein amide C=O stretching vibrations, amide II absorption arise from amide N–H bending vibrations and C–N stretching vibrations (60% and 40% contribution to the peak, respectively), and the amide III peak is complex, consisting of the components from C–N stretching and N–H in plane bending from amide linkages, as well as the absorptions arising from wagging vibrations from CH_2 groups in the glycine backbone and proline side-chains (Sionkowska et al., 2004). Amide III peak has an absorption at 1240 cm^{-1}, with two other smaller peaks at 1340 and 1160 cm^{-1}. The characteristic absorption band at 1400 cm^{-1} is caused by COO^- group.

The spectra of collagen casting membrane from its HFP/TFA solution are quite similar to those of raw collagen as shown in Fig. 3. But the amide I, II and III bands were transferred from 1660, 1550 and 1240 cm^{-1} of raw collagen to 1640, 1540 and 1290 cm^{-1}, respectively. The characteristic absorption band of COO^- was also trans-

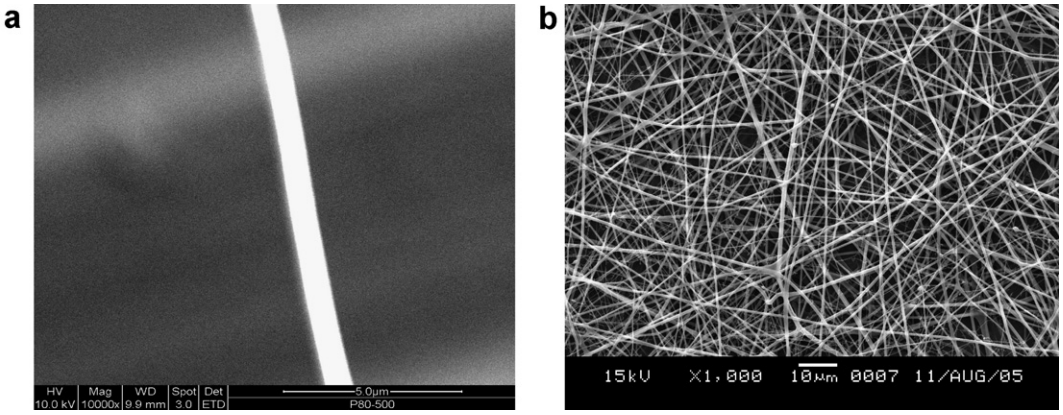

Fig. 2. SEM micrographs of electrospun collagen–chitosan single fiber and membrane with chitosan content of 50%. (a) A single fiber; (b) membrane.

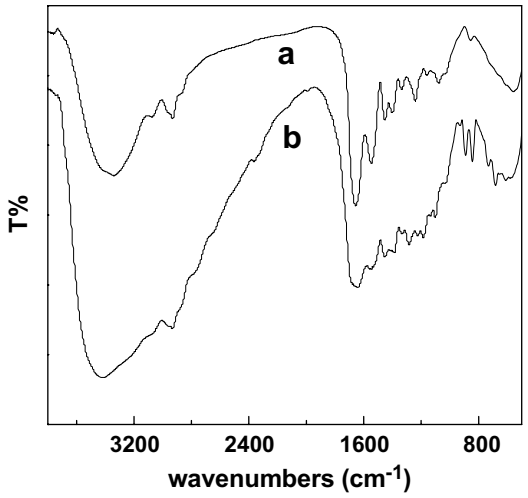

Fig. 3. FT-IR spectra of collagen. (a) raw collagen; (b) collagen casting membrane.

ferred to 1390 cm^{-1}. This implied that hydrogen bonds may be formed between collagen and the solvent.

Fig. 4 shows the FT-IR spectra of raw chitosan and its casting membrane from its HFP/TFA solution. In Fig. 4a, the characteristic absorption bands at 1660, 1600 and 1260 cm^{-1} represent the amide I band, amide N–H group bending vibration and amide III band, respectively. The characteristic absorption bands at 1660 cm^{-1} and 1600 cm^{-1} overlap each other, moreover, no amide II band can be seen and the characteristic absorption peak of amide III band at 1260 is weak in intensity. All these suggest that chitosan is a partially deacetylated product. The FT-IR spectra of chitosan casting membrane shown in Fig. 4b reveal slightly difference with those of raw chitosan. The amide I absorption margin with characteristic absorption band of amide N–H group and shown a wide absorption at 1610 cm^{-1}. The characteristic absorption peak of amide III band at 1260 is increased in intensity. A new characteristic absorption peak appears at 1400 cm^{-1}, which represent the $–COO^-$ band. This means that amine salts can be formed between chitosan and TFA. Hasegawa had reported that TFA can form salts with the amino groups of chitosan (Hasegawa et al., 1992). The formation of salt destroys the strong interaction between the chitosan molecules. Comparing with raw chitosan, one of characteristic absorption peaks representing C–O–C bands at 1160 cm^{-1} disappears. All these imply that new hydrogen bonds or interactions can be formed between chitosan and HFP/TFA mixtures.

3.2.2. FT-IR spectra of electrospun collagen–chitosan complex nanofibers

The FT-IR spectra of electrospun collagen depict characteristic absorption bands at 1640, 1540 and 1250 cm^{-1}, which represent the amide I, II and III bands of collagen. Another peak is also seen at 1330 cm^{-1} near the amide III characteristic absorption band as shown in Fig. 5a. Comparing with raw collagen and collagen casting membrane, only small modifications can be seen in the IR spectrum of electrospun collagen.

Comparing with raw chitosan and dissolved chitosan, electrospun chitosan displays new characteristic absorption bands at 1680 and 1540 cm^{-1} which represent the amide I, II characteristic absorption bands, respectively. The amide III band disappears and only another peak is seen at 1320 cm^{-1} as shown in Fig. 5e. The amide I absorption band and the amide II absorption band suggest that electric charge in electrospinning can facilitate the reaction between $–NH_2$ of chitosan and –COOH of TFA partially. The disappearance of the amide III band at 1250 means that new intermolecular interactions can be formed itself or between chitosan and HFP/THF mixtures in electrospinning.

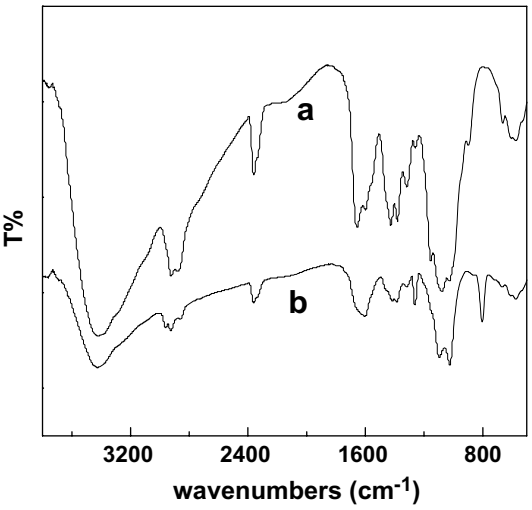

Fig. 4. FT-IR spectra of chitosan. (a) raw chitosan; (b) chitosan casting membrane.

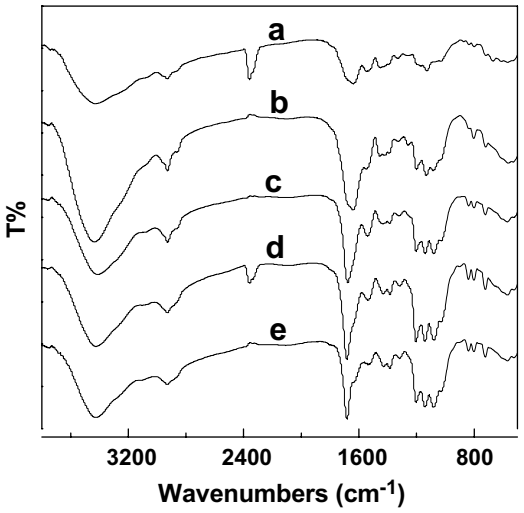

Fig. 5. FT-IR spectra of electrospun collagen–chitosan complex nanofibers with different chitosan content. (a) 0%; (b) 20%; (c) 50%; (d) 80%; (e) 100%.

FT-IR spectra corresponding to electrospun collagen–chitosan complex nanofibers are also shown in Fig. 5. These spectra are quite similar each other owing to their same main functional groups, nevertheless various small modifications are revealed in the spectra with the change of chitosan content. Electrospun collagen, chitosan and their blends display characteristic absorption bands between 3400 cm^{-1} and 3450 cm^{-1}, which represent the –OH group and the $–NH_2$ group in free as well as in amide form (i.e., N–H stretching from CO–NH portion) in collagen and chitosan. The position of characteristic absorption bands between 3400 and 3450 cm^{-1} in blends are shifted with various chitosan content in electrospun collagen–chitosan nanofibers as shown in Table 1.

With chitosan content increasing from 0%, 20%, 50%, 80% to 100%, of electrospun blends, the amide I characteristic absorption bands shift from 1640 to 1680 cm^{-1}. The intensity of amide II peak at 1550 cm^{-1} vary with chitosan content, but it is not in proportion to chitosan content and it is especially week at chitosan content of 20%. That means the amide N–H bending vibrations and C–N stretching vibrations are prohibited, which may be caused by new formed hydrogen bonds between collagen and chitosan. Moreover, the amide III characteristic absorption peak is seen at 1260 cm^{-1} with another peak at 1320 cm^{-1} at chitosan content of 20% and only leave one absorption peak at 1320 cm^{-1} when chitosan content increased to 50% and 80% in the electrospun fibers.

The interactions between collagen and chitosan may occur by hydrogen bonds formation. The –OH groups and $–NH_2$ groups in collagen are capable of forming hydrogen bonds with –OH and $–NH_2$ groups in chitosan. Moreover, the ═C═O groups and $–NH_2$ groups in collagen may also form hydrogen bonds with –OH and $–NH_2$ groups in chitosan. Additionally, ionic bonds may be formed between collagen and chitosan. These molecules are capable of forming complex with oppositely charged ionic polymers, especially the cationic polysaccharide chitosan and anionic –COOH group in collagen. These interactions may form polyanionic–polycationic complex (Sionkowska et al., 2004). But the evidence of FT-IR spectra here can not indicate the formation of new polyanionic–polycationic complex between collagen and chitosan obviously, owing to their same main functional groups.

3.4. Thermal properties

Fig. 6 shows the DSC thermograms of collagen, chitosan and their blends. The characteristic endothermic peaks

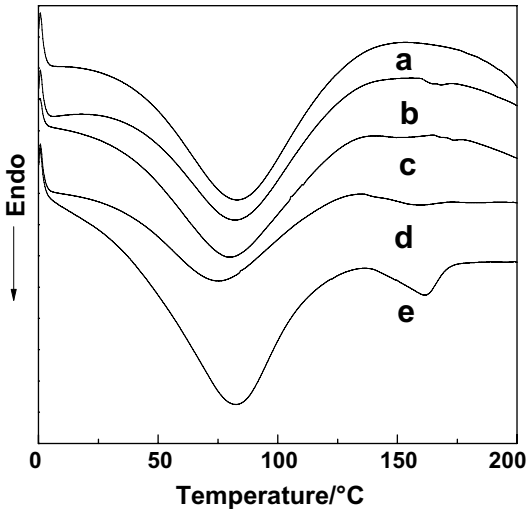

Fig. 6. DSC thermograms of electrospun collagen–chitosan complex nanofibers with different chitosan content. (a) 100%; (b) 80%; (c) 50%; (d) 20% (e) 0%.

in Fig. 6 have often been termed as dehydration temperature (T_D) due to the water bonded to collagen and chitosan molecules. The DSC data are listed in the Table 2. T_D for collagen and chitosan blends is lower than T_D for the single component. The enthalpy ΔH_D for the blend is also lower than the enthalpy for single component. The facts confirm the existence of interactions between collagen and chitosan. For single components, the enthalpy characterizes interactions between collagen–collagen, collagen–H_2O, chitosan–chitosan and chitosan–H_2O. In the blends, these interactions are replaced by interactions between collagen and chitosan partly. It can be drawn a conclusion that the formation of hydrogen bonds between two different macromolecules competes with the formation of hydrogen bonds between molecules of the same polymer (Sionkowska, 2003).

3.5. Mechanical properties

All the electrospun collagen–chitosan fibers shown the brittle mechanical behavior except the one with chitosan content of 20%, which gives about 30 times longer elongation at break comparing with other electrospun collagen–chitosan fibers with different chitosan content. Moreover, the average tensile strength and the Young's modulus of fibers increase greatly and reach a maximum at chitosan content of 50% in the blends. That means some intermolecular interactions exist in the blends.

Table 1
The position of –OH group and the –NH group characteristic absorption bands of electrospun collagen–chitosan fibers with different chitosan content

Chitosan content (%)	0	20	50	80	100
Absorption band position (cm^{-1})	3423	3434	3412	3424	3423

Table 2
Thermal properties of electrospun collagen–chitosan complex fibers with different chitosan content

Chitosan content (%)	0	20	50	80	100
T_D (°C)	82.35	75.20	79.49	82.16	82.95
ΔH_D (J/g)	218.9	182.9	188.0	192.0	217.3

The average ultimate tensile strength, the average ultimate tensile elongation and the average Young's modulus of the single electrospun collagen–chitosan nanofibers with various chitosan content were tested and summarized in Table 3. Fig. 7 characters the relations between the average ultimate tensile elongation and chitosan content while Fig. 8 characters the relations between the average ultimate tensile strength and chitosan content. As the single fiber collection is very difficulty for the chitosan content higher than 80%, the mechanical properties tested here are limited to 80% chitosan content only.

In collagen, the main structure of polypeptide is composed of the helix of α chains and extended β chains of peptides. The helix of α chain can be transformed into extended β chain when they are drawn in humidity (Wang & Sun, 1982). Type I collagen fibrils are composed of two α_1 chains and one α_2 chain and intense hydrogen bonds and Van der Waals forces exist among these peptide chains. Type I collagen fiber should have appropriate tensile elongation owing to helix α chains, but intense interactions in three α chains of peptides can prevent helix α chains stretching. So the tensile elongation of collagen fiber is low as shown Fig. 7. With a small amount of chitosan added in the collagen, such as 20%, the intermolecular interactions between collagen and chitosan can weaken the hydrogen bonds and the interactions in the three chains of peptides in collagen, which can result in the chains of peptides stretching more facilely. So the tensile elongation of collagen–chitosan fiber is increased greatly. When chitosan content is increased further to 40% and 50% in the electrospun fibers, the average tensile elongation of single collage–chitosan complex fibers decrease obviously, while the average tensile strength and the Young's modulus of fibers increase greatly and reach a maximum as shown in Fig. 8 and Table 3. The reason can be due to the intense intermolecular interactions or some physical property change such as crystalinity or molecular chains orientation in the collagen–chitosan complex fibers.

The X-ray diffraction analyses are shown in Fig. 9. The raw chitosan shows two peaks at around 9.5°and 19.5°in Fig. 9A as curve b. The two peaks are related to two different types of crystals: crystal (1) and crystal (2) (Samuels, 1981). In the case of the raw collagen, one reflection at around 7.5° and a broad band at around 20.5°are observed in Fig. 9A as curve a. After electrospinning, the collagen, chitosan and their complex fibers show typical amorphous broad peak at around 20.5° that means both collagen and chitosan molecular chains can not crystallized during electrospinning and give similar amorphous structure in nanofibers.

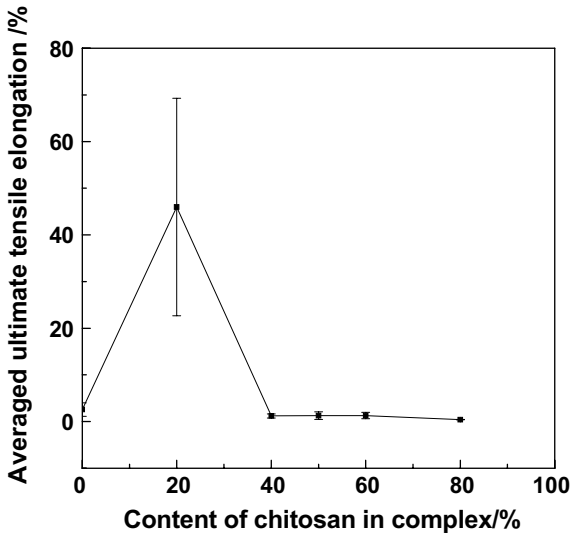

Fig. 7. Relations between averaged ultimate tensile elongation of fibers and chitosan content.

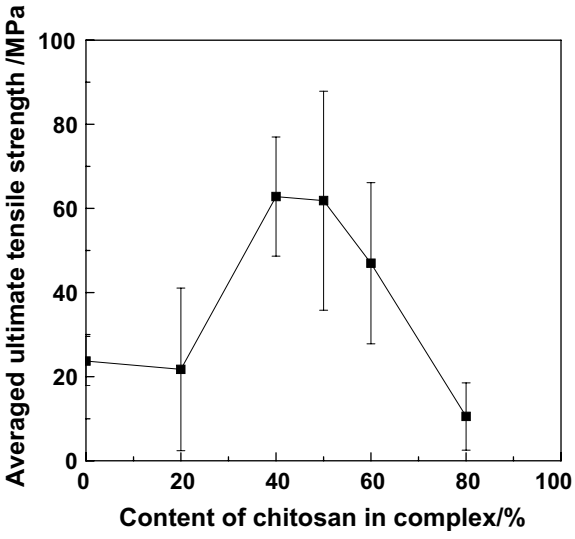

Fig. 8. Relations between averaged ultimate tensile strength of fibers and chitosan content.

So the mechanical properties difference of electrospun collagen–chitosan fibers is mainly caused by the component change and intermolecular interactions. So the stronger ultimate strength and Young's modulus of collagen–chitosan nanofiber at chitosan content of 40–60% is

Table 3
Tensile properties of electrospun collagen–chitosan complex single fibers with different chitosan content

Chitosan content (%)	0	20	40	50	60	80
Average ultimate elongation (%)	2.6 ± 1.4	46.0 ± 23	1.2 ± 0.4	1.3 ± 0.8	1.3 ± 0.7	0.4 ± 0.04
Average ultimate strength (MPa)	23.7 ± 5.8	21.7 ± 19.3	62.8 ± 14.1	61.8 ± 26.0	47.0 ± 19.1	10.5 ± 8.0
Average Young's module (MPa)	1371 ± 225	1611 ± 793	5966 ± 2137	6801 ± 3256	4159 ± 1195	3601 ± 485
Average diameter of fibers (μm)	7.8 ± 5.0	4.4 ± 1.2	6.8 ± 12.1	5.6 ± 4.0	3.4 ± 0.8	9.1 ± 1.4 ($n = 3$)

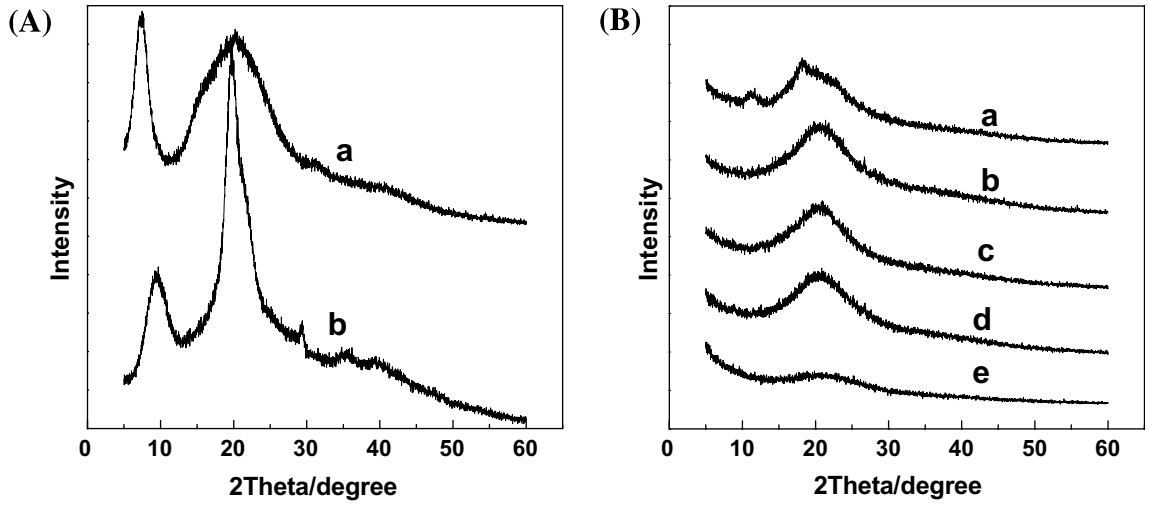

Fig. 9. X-ray diffraction patterns. (A) raw materials: (a) collagen; (b) chitosan. (B) electrospun nanofibers with different chitosan content (a) 100%; (b) 80%; (c) 50%; (d) 20%; (e) 0%.

caused by the intense intermolecular interactions between collagen and chitosan. Moreover, the ionic bonds may be formed between collagen and chitosan besides hydrogen bonds. The interactions may also form polyanionic–polycationic complex, which result in the excellent tensile strength and Young's modulus of fibers. But intense molecular interactions in collagen and chitosan complex fibers may restrain the deformation of collagen molecules. All these result in the poor tensile elongation of single collage–chitosan complex fibers.

When chitosan content increased to 80% in the complex nanofibers, the mechanical properties show a more brittle mechanical behavior.

4. Conclusion

The collagen–chitosan complex nanofibers were prepared here by electrospinning. FT-IR, DSC and the mechanical measurements of single nanofiber results pointed out interactions in electrospun collagen–chitosan complex fibers. Collagen may form different types of hydrogen bonds with chitosan: between carbonyl group, hydroxyl group, amino group of collagen and hydroxyl group, amino group, carbonyl group of chitosan. The formation of hydrogen bonds between two different macromolecules competes with the formation of hydrogen bonds between molecules of the same polymer. Additionally, ionic bonds may be formed between collagen and chitosan, especially when chitosan content is near collagen content in electrospun fibers. From these results we can conclude that electrospun collagen and chitosan are miscible at the molecular level and that electrospinning of the collagen and chitosan blends may give the possibility of producing new materials for potential biomedical applications.

Acknowledgements

This research was supported by National Nature Science Foundation of China under the Grant 30570503 and Shanghai Sci. & Tech. Committee China under the Grants 05DJ14006 and 05PJ14013.

References

Alberts, B., Bray, D., Lewis, J., Raff, M., Roberts, K., & Watson, J. D. (1994). *Molecular Biology of the Cell*. Garland: Garland Publishing.

Chen, R. N., Wang, G. M., Chen, C. H., Ho, H. O., & Sheu, M. T. (2006). Development of N, O-(carboxymethyl) chitosan/collagen matrixes as a wound dressing. *Biomacromolecules, 7*, 1058–1064.

Chen, Z. G., Mo, X. M., & Qing, F. L. (2006). Electrospinning of chitosan collagen complex: To mimic the native extracellular matrix. *Tissue Engineering, 12*, 1074.

Chen, Z. G., Mo, X. M., & Qing, F. L. (2007). Electrospinning of collagen–chitosan complex. *Materials Letters, 61*, 3490–3494.

Cui, F. Z., & Feng, Q. L. (2004). *Biomaterials science*. Beijing: Tsinghua University Press.

Domard, A., & Taravel, M. N. (1995). Collagen and its interaction with chitosan: II. Influence of the physicochemical characteristics of collagen. *Biomaterials, 16*, 865–871.

Gomathi, K., Gopinath, D., Ahmed, M. R., & Jayakumar, R. (2003). Quercetin incorporated collagen matrices for dermal wound healing processes in rat. *Biomaterials, 24*, 2767–2772.

Hasegawa, M., Isogai, A., Onabe, F., & Usuda, M. (1992). Dissolving states of cellulose and chitosan in trifluoroacetic acid. *Journal of Applied Polymer Science, 45*, 1857–1863.

Hirano, S., Zhang, M., Nakagawa, M., & Miyata, T. (2000). Wet spun chitosan-collagen fibers, their chemical *N*-modifications and blood compatibility. *Biomaterials, 21*, 997–1003.

Huang, Y., Onyeri, S., Siewe, M., Moshfeghian, A., & Madihally, S. V. (2005). In vitro characterization of chitosan–gelatin scaffolds for tissue engineering. *Biomaterials, 26*, 7616–7627.

Huang, Z. L., & Jiang, G. J. (2006). Manufacture of gelatin/chitosan wound dressing and experimental study on its biological evaluation. *Tissue Engineering, 12*, 1070–1071.

Huang, Z. M., Zhang, Y. Z., Kotaki, M., & Ramakrishna, S. (2003). A review on polymer nanofibers by electrospinning and their applications

in nanocomposites. *Composites Science and Technology, 63*, 2223–2253.

Jin, H. J., Fridrikh, S. V., Rutledge, G. C., & Kaplan, D. I. (2002). Electrospinning bombyx mori silk with poly (ethylene oxide). *Biomacromolecules, 3*, 1233–1239.

Kaminska, A., & Sionkowska, A. (1996). Effect of UV radiation on the infrared spectra of collagen. *Polymer Degradation and Stability, 51*, 19.

Khil, M. S., Cha, D. I., Kim, H. Y., Kim, I. S., & Bhattarai, N. (2003). Electrospun nanofibrous polyurethane membrane as wound dressing. *Journal of Biomedical Materials Research Part (B), 67*, 675–679.

Ky, D., Liu, C. K., Marumoto, C., Castaneda, L., & Slowinska, K. (2006). Electrochemical Time-of-Flight in cross-linked collagen matrix solution: Implications of structural changes for drug delivery systems. *Journal of Controlled Release, 112*, 214–222.

Laurencin, C. T., Ambrosio, A. M. A., Borden, M. D., & Cooper, J. A. Jr., (1999). Tissue engineering: Orthopedic applications. *Annual Review of Biomedical Engineering, 1*, 19–46.

Lee, S. B., Kim, Y. H., Chong, M. S., & Lee, Y. M. (2004). Preparation and characteristics of hybrid scaffolds composed of b-chitin and collagen. *Biomaterials, 25*, 2309–2317.

Ma, L., Gao, C. Y., Mao, Z. W., Zhou, J., Shen, J. C., Hu, X. Q., et al. (2003). Collagen/chitosan porous scaffolds with improved biostability for skin tissue engineering. *Biomaterials, 24*, 4833–4841.

Marois, Y., Chakfé, N., Deng, X. Y., Marois, M., How, T., King, M. W., et al. (1995). Carbodiimide cross-linked gelatin: a new coating for porous polyester arterial prostheses. *Biomaterials, 16*, 1131–1139.

Matthews, J. A., Wnek, G. E., Simpson, D. G., & Bowlin, G. L. (2002). Electrospinning of collagen nanofibers. *Biomacromolecules, 3*, 232–238.

Mo, X. M. (1997). The study of chitosan and gelatin complex. *Acta Polymeric Sinica, 46*, 222–226.

Samuels, R. J. (1981). Solid state characterization of the structure of chitosan films. *Journal of Polymer Science Part B: Polymer Physics, 19*, 1081.

Silver, F. H., & Christiansen, D. L. (1999). *Biomaterials Science and Biocompatibility*. New York: Springer-Verlag.

Sionkowska, A., Wisniewski, M., Skopinska, J., Kennedy, C. J., & Wess, T. J. (2004). Molecular interactions in collagen and chitosan blends. *Biomaterials, 25*, 795–801.

Sionkowska, A. (2003). Interaction of collagen and poly (vinyl pyrrolidone) in blends. *European Polymer Journal, 39*, 2135–2140.

Taravel, M. N., & Domard, A. (1993). Relation between the physicochemical characteristics of collagen and its interactions with chitosan: I. *Biomaterials, 14*, 930–938.

Taravel, M. N., & Domard, A. (1996). Collagen and its interactions with chitosan: III. Some biological and mechanical properties. *Biomaterials, 17*, 451–455.

Wang, J. S., & Sun, K. (1982). *Theory of dyeing and finishing* (vol. 1). Beijing: Textile industry press.

Wang, X. H., Li, D. P., Wang, W. J., Feng, Q. L., Cui, F. Z., Xu, Y. X., et al. (2003). Cross-linked collagen/chitosan matrix for artificial livers. *Biomaterials, 24*, 3213–3220.

Webster, T. J., Waid, M. C., McKenzie, J. L., Price, R. L., & Ejiofor, J. U. (2004). Nano-biotechnology: Carbon nanofibres as improved neural and orthopaedic implants. *Nanotechnology, 15*, 48–54.

Zeng, J., Xu, X., Chen, X., Liang, Q., Bian, X., Yang, L., et al. (2003). Biodegradable electrospun fibers for drug delivery. *Journal of Controlled Release, 92*, 227–231.